Dalton Transactions

Accepted Manuscript

Dalton Transactions

ARTICLE

Exploring the Reactivity of Manganese(III) Complexes with Diphenolate-diamino Ligands in *rac*-Lactide Polymerization

Received 00th January 20xx,
Accepted 00th January 20xx

DOI: 10.1039/x0xx00000x

www.rsc.org/

Pargol Daneshmand, Frank Schaper*

Manganese(III) complexes of tetradentate diphenolate-diamino ($NNOO^{2-}$) ligands were prepared from aerobic reaction of $MnCl_2$ with the respective ligands in basic methanolic solution. Methoxide complexes (NNOO)Mn(OMe)$(MeOH)_{0-1}$ were obtained for three ligands, while others only provided the respective chloride complexes (NNOO)Mn(Cl)(MeOH). Complexes were analyzed by X-ray diffraction studies and octahedral complexes showed evidence of Jahn-Teller distortions. Magnetic moments determined in MeOD were indicative of high-spin Mn(III)-d^4 complexes (μ_{eff} = 4.2 – 4.6 μ_B). Methoxide complexes were active in the coordination-insertion polymerization of *rac*-lactide (130 °C, 0.33 – 1.0 mol-% catalyst loading) to yield atactic polylactic acid with moderate molecular weight control. Polymerization activity was reduced, but not suppressed by the presence of protic impurities. Chloride complexes showed less activity and only in the presence of external alcohol, indicative of an activated-monomer mechanism.

Introduction

Interest in bio-degradable polymers and materials obtained from renewable resources[1, 2] sparked a large number of investigations in the coordination-insertion polymerization of *rac*-lactide.[3-16] Catalysts with desirable characteristics such as high activity, isoselectivity, perfect molecular weight control, absence of side reactions or chemical robustness have been reported, even though combining all of these in one catalytic system still remains challenging. Most of the investigated catalyst systems are based on metals with an empty *d*-shell (group 1-4 and rare earth metals)[3, 7, 13-23] or a filled *d*-shell (Zn, group 13-14).[4-6, 11, 14, 15, 24, 25]

Of catalysts based on mid-range transition metals, only iron[26-42] and copper[43-54] have been studied in somewhat more detail. Copper catalysts originally showed low to moderate activities,[43-47] but choosing the right ligand system recently provided catalysts with very high activities,[48-54] and even in one case isoselectivity.[54] Catalyst based on Cr,[55] Mn,[38, 56, 57] Ni,[44, 58-60] or Co,[57] remain curiously understudied. Of the three studies employing Mn catalysts for lactide polymerization, two relied on the use of manganese salts, such as $MnCl_2$ or $Mn(OAc)_2$, acting essentially as simple Lewis acids.[56, 57] Idage et al. employed a Mn(III) salen chloride complex and achieved moderate activities and good polymer molecular weight control.[38] A coordination-insertion mechanism was reported, although no nucleophile other than the ligand was present.

Given the promising activities and the limited amount of studies with Mn-based catalysts, we decided to further explore the performance of air- and moisture-stable manganese complexes in lactide polymerization. In particular, we were interested in complexes of type **A** (Scheme 1), which are designed to follow a coordination-insertion mechanism. To provide stability at ambient atmosphere, Mn(III) complexes were targeted, which required a dianionic spectator ligand. Diamino-diphenolate ligands are readily synthesized, can be easily modified, provide good hydrolytic stability and have been introduced in lactide polymerization by Carpentier for group 3 metals,[18] by Kol for group 4,[61] by Gibson for group 13,[62] and by Cui and Mountford for lanthanides.[63, 64] We thus explored ligands **1** and **2** as spectator ligands for Mn-catalysed lactide polymerizations.

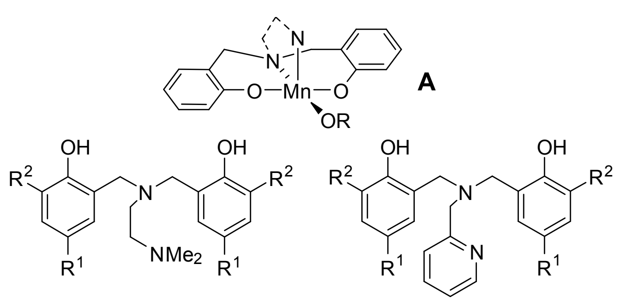

1a : $R^1 = R^2 = t$Bu
1b : $R^1 = R^2 =$ Cl
1c : $R^1 = t$Bu, $R^2 =$ Me

2a : $R^1 = R^2 = t$Bu
2b : $R^1 = R^2 =$Cl
2c : $R^1 = t$Bu, $R^2 =$ Me

Scheme 1

Centre in Green Chemistry and Catalysis, Department of chemistry, Université de Montréal, C. P. 6128 Succ. Centre-Ville, Montréal, QC, H3T 3J7, Canada. Email: Frank.Schaper@umontreal.ca

Electronic Supplementary Information (ESI) available: [Additional details on polymerization reactions, MALDI-spectra, X-ray structure determinations (CIF).]. See DOI: 10.1039/x0xx00000x

Results and Discussion

Synthesis. Ligands **1** and **2** were prepared with slight variations of literature protocols (see Experimental Section). Manganese(III) complexes with ligands identical or similar to those employed here have been reported with the ancillary ligand being carboxylates,[65-68] azide or thiocyanate,[69, 70] or planar, bidentate ligands such as acetylactonate.[68, 71] Since in all cases octahedral complexes had been reported, initial attempts concentrated on the preparation of complexes containing a chelating alcohol, such as pyridyl methoxide or dimethylamino ethoxide, to provide octahedral complexes and to suppress potential β-H elimination reactions in the presence of an open coordination site. Consistent colour changes to red-brown in these reactions seem to indicate ligand coordination to manganese, but despite numerous attempts and variations in Mn source, solvent, base and temperature, neither crystalline material nor powders showing correct combustion analyses could be obtained (Scheme 2).

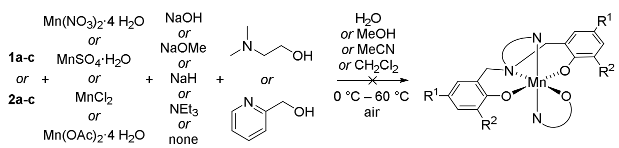

Scheme2

A recurrent trend in the obtained combustion analyses were low nitrogen values, indicating a lack of coordination of the chelating alcohol. Replacement of the chelating alcohol by a mixture of methoxide/acetonitrile gave indeed small amounts of a methoxide complex, which did not, however, contain acetonitrile. In an optimized procedure, ligands **1a** and **1b** were then reacted with $MnCl_2$ and 2 equiv NaOH in methanol and provided the five-coordinated methoxide complexes **3a** and **3b** (Scheme 3). Reactions of **2a** and **2b** under the same conditions did not yield crystalline material and the base was switched to sodium methoxide. Reaction of **2a** with $MnCl_2$ in the presence of two equivalents of NaOMe provided only the chloride complex **4a**·MeOH. To encourage chloride/methoxide exchange, the reaction was repeated with four equivalents of NaOMe and yielded the methoxide complex **5a**·MeOH. Both complexes were obtained as hexacoordinated complexes with an additional methanol ligand.

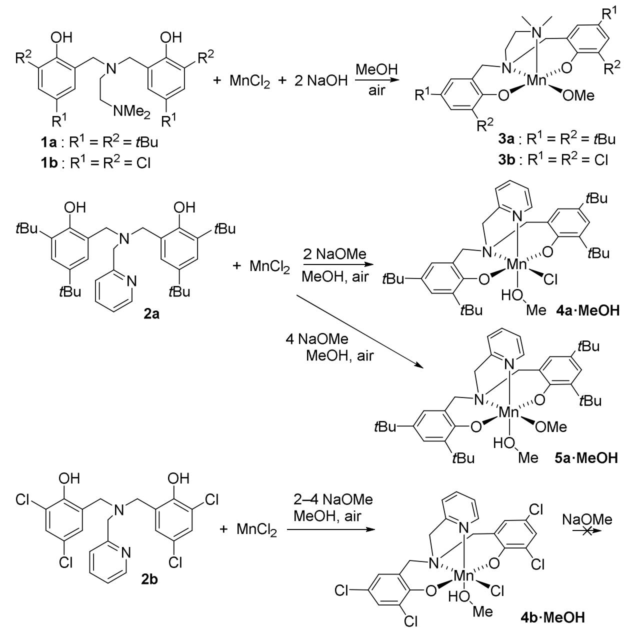

Scheme 3

Reactions of ligand **2b** with $MnCl_2$ and 2-4 equiv of sodium methoxide under various reaction temperatures did not provide a methoxide complex, but the chloride complex **4b**·MeOH. Reaction of the isolated chloride complex **4b**·MeOH with sodium methoxide was likewise unsuccessful (Scheme 3). Variation of the manganese source to $MnBr_2$ or MnI_2 did not provide any improvement, neither did variation of the base (NaOH or NEt_3) or of the solvent. Ligands **1c** or **2c** failed to produce any isolable or characterizable material, regardless of the conditions employed.

UV/vis-spectra. In addition to high-intensity transitions below 300 nm, all Mn complexes display several peaks in the visible region with intensities indicative of charge-transfer transitions (Fig. 1). Based on the hypsochromic displacement observed when the *tert*-butyl substituents in **3a** (330, 381 and 512 nm) are replaced by chloride in **3b** (293, 370, and 484 nm) or, likewise, in **4a**·MeOH (376 and 518 nm) and **4b**·MeOH (360 and 470 nm), we tentatively assign these as MLCT transitions from MeO^- or Cl^- to Mn. Bathochromic shifts of the two low-energy transitions when replacing the Mn-bound chloride in **4a**·MeOH against methoxide in **5a**·MeOH (376/518 nm and 410/540 nm, respectively) are in agreement with this assignment.

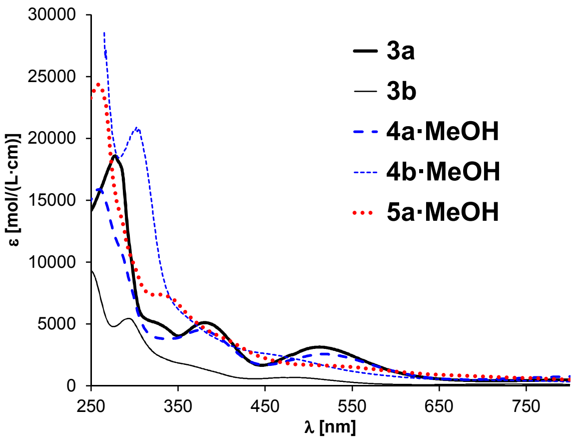

Figure 1. UV/vis spectra in methanol of manganese complexes **3a** (solid bold), **3b** (solid thin), **4b**·MeOH (dashed bold), **4b**·MeOH (dashed thin) and **5a**·MeOH (dotted).

Magnetic moments. Magnetic susceptibilities were determined using the Evans NMR method at ambient temperature in MeOD and yielded the expected values for high-spin Mn(III) with $\mu_{eff} = 4.2 – 4.6\ \mu_B$.[72, 73]

Solid-state structures. Crystals for diffraction studies were obtained for all complexes, but **3b** (Fig. 2, Table 1). The complexes show a wide diversity of conformations due to the flexibility of the tetradentate ligand. In **3a**, the two oxametallacycles formed by the phenolate ligands display a boat-conformation, with one aryl ring orientated towards the dimethylamino ligand (endo), the other oriented away from this ligand (exo). The exo-oriented aryl ring most likely prevents coordination of a sixth ligand. Complex **3a** has a geometry intermediate between square-pyramidal and trigonal-bipyramidal ($\tau = 0.4$), but can be considered square-pyramidal with N2 in the apical position for the following discussion. The remaining complexes complete octahedral geometry by coordination of methanol solvent. The equatorial plane contains the phenolate oxygen atoms O1 and O2 and the nitrogen bridgehead atom N1 with Mn-O distances of 1.86 – 1.94 Å and Mn-N1 distances of 2.13 – 2.18 Å (Table 1). The N2 atom of the pyridine ligand is found in the apical position with Mn-N2 distances of 2.22 – 2.34 Å, slightly longer than Mn-N1 due to Jahn-Teller distortions expected for high-spin Mn(III) complexes. In **4a**·MeOH and **5a**·MeOH, the methanol ligand is found in the apical position trans to N2, while in **4b**·MeOH, the chloride ligand is found trans to N2, with an increased Mn-Cl bond length (2.498(1) Å in **4b** vs. 2.370(2) in **4a**), again due to Jahn-Teller distortions. Similar Mn-Cl distances are observed in octahedral Mn(III) chloride complexes with salen and related ligands, which force the chloride ligand in an apical position due to ligand planarity (Mn-Cl = 2.43 – 2.68 Å, n = 41).[74] As expected, the methanol ligand shows the reversed trend with a shorter Mn-O distance in **4b**·MeOH (2.086(2) Å, trans to N1) then in **4a**·MeOH or **5a**·MeOH (2.257(5) and 2.273(3) Å, trans to N2).

There is no obvious steric explanation for the placement of the anionic vs. methanol ligand. Neither does it correlate with the conformation of the oxametallacycles (Table 1), i. e. a half-chair/endo-boat conformation is observed both for **5a**·MeOH and **4b**·MeOH. The only structural correlation consists in the evidence of π-stacking to pyridine: a bending of pyridine towards the phenolate ring in **4a**·MeOH and **5a**·MeOH (Fig. 2) is indicative of weak π-stacking interactions between the electron-rich bis-*tert*-butyl phenol and pyridine (aryl-aryl angle = 32°, d(atom-plane) 2.9-4.3 Å). As a consequence, the pyridine ring is no longer perpendicular to the equatorial plane (67°). In **4b**·MeOH, there is no approach of the pyridine ring towards the less electron-rich dichlorophenolate (aryl-aryl angle = 51°) and the pyridine ring remains perpendicular to the equatorial plane (88°). Placement of chloride trans to pyridine in **4b**·MeOH might thus be related to better π-interaction of the pyridine with the metal d-orbitals.

Table 1. Selected bond distances [Å] and bond angles [°] from X-ray diffraction studies

	3a	**5a**·MeOH	**4a**·MeOH	**4b**·MeOH
Mn-OAr	1.896(2), 1.926(2)	1.884(2), 1.894(2)	1.895(4), 1.936(4)	1.858(2), 1.871(2)
Mn-N1	2.125(2)	2.132(3)	2.178(5)	2.142(2)
Mn-N2	2.254(2)	2.342(3)	2.226(5)	2.224(2)
Mn-X	1.856(2) (OMe)	1.896(3) (OMe)	2.370(2) (Cl)	2.498(1) (Cl)
Me-O(H)Me		2.273(3)	2.262(5)	2.086(2)
ArO-Mn-OAr	151.54(7)	176.06(10)	171.4(2)	176.65(8)
ArO-Mn-N1	89.29(7), 90.18(7)	88.01(10), 90.81(10)	88.8(2), 91.1(2)	88.54(8), 94.05(8)
N1-Mn-Y [a]	174.83(8)	176.50(11)	174.7(1)	166.45(8)
Ring conformations	exo-boat, endo-boat	half-chair, endo-boat	endo-boat, endo-boat	half-chair, endo-boat

[a] Y (ligand trans to N1) = O3 (OMe^-; **3a**, **5a**·MeOH), Cl1 (**4a**·MeOH), O3 (MeOH; **4b**·MeOH)

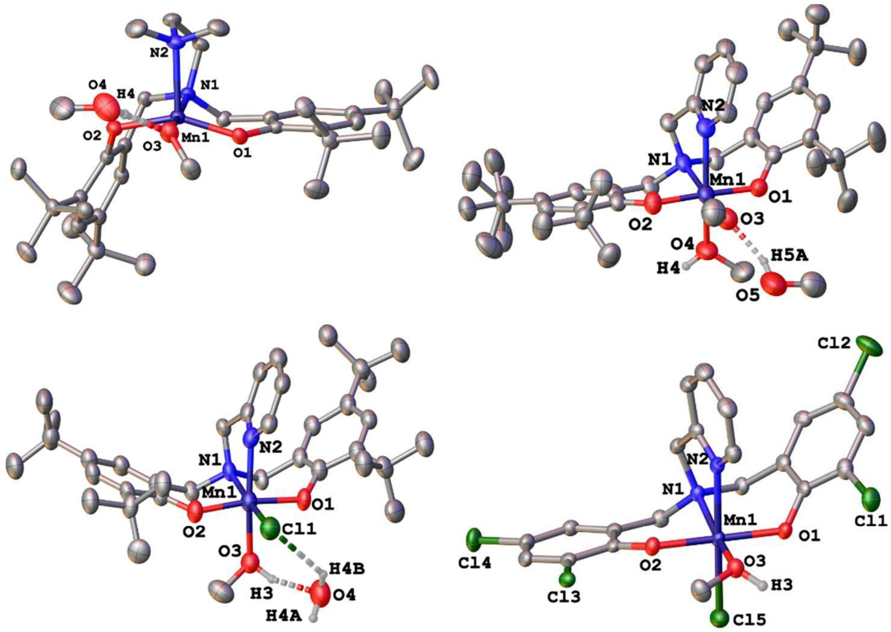

Figure 2. X-ray structure of **3a** (top left), **5a**·MeOH (top right), **4a**·MeOH (bottom left), and **4b**·MeOH (bottom right). Thermal ellipsoids are drawn at 50% probability. Hydrogen atoms (except those on methanol or water molecules) omitted for clarity.

Lactide polymerization. Alkoxide complexes **3a**, **3b** and **5a**·MeOH were tested for the polymerization of *rac*-lactide in solution, but proved to be inactive in dichloromethane at ambient temperature or toluene at 70 °C. In molten monomer at 130 °C all catalysts were moderately active and maximum conversion was reached in 4 – 6 hours (Tables 2 and S1). Polymerizations with **3a** showed evidence for catalyst decomposition: appr. 50% conversion was reached after 2 h, but prolongation of the polymerization time did not lead to higher conversions (with exception of one outlier experiment). Conversion was independent from catalyst concentration and decomposition is likely caused by thermal degradation of the active species rather than by impurities in the monomer. Irregular and large disagreements between calculated and observed molecular weights indicate chain termination reactions, in line with thermal degradation of the catalyst. Complex **3b** likewise did not show a notable difference in conversion between 2 and 4 h of reaction time, indicating that the active species was largely decomposed at this time. In contrast to **3a**, matching calculated and observed molecular weights and polydispersities of 1.2 – 1.3 indicate improved polymerization control despite catalyst degradation. Increased yields at higher catalyst loadings, together with the better polymer weight control, indicate a slightly higher thermal stability of **3b**.

Table 2. *Rac*-lactide polymerization with **3a**, **3b** and **5a·MeOH** [a]

Catalyst	Lactide : Mn	Reaction time / h	Conversion · 100	M_n (calc.) · mol/kg [b]	M_n (GPC) · mol/kg [c]	M_w/M_n
3a	100:1	2	49	3.5	1.5	1.1
3a	100:1	4	52	4.0	2.5	1.2
3a	100:1	6	47	3.5	6.5	1.4
3a	100:1	6	91	6.5	3.0	1.3
3a	300:1	2	53	11.0	11.0	1.3
3a	300:1	4	43	9.5	2.0	1.1
3a	300:1	6	51	11.0	29.0	1.5
3a	300:1	6	56	12.0	2.5	1.2
3b	100:1	4	71	10.5	11.0	1.3
3b	100:1	6	81	11.5	13.5	1.3
3b	200:1	4	38	11.0	7.5	1.2
3b	200:1	6	48	14.0	11.0	1.2
5a·MeOH	100:1	2	41	3.0	3.5	1.1
5a·MeOH	100:1	4	90	6.5	5.0	1.5
5a·MeOH	200:1	2	51	7.5	2.0	1.1
5a·MeOH	200:1	4	88	13.0	15.5	1.4
5a·MeOH	300:1	2	56	12.0	12.0	1.3
5a·MeOH	300:1	4	88	19.0	16.0	1.6

[a] Conditions: 130 °C, sealed tube under N_2. [b] Calculated from $m_{lactide}/(n_{catalyst}+n_{alcohol})\cdot$conversion$+M_{MeOH}$. $n_{alcohol}$ was determined from the elemental analysis, since in all complexes but **3a** co-crystallized solvent was lost on drying, while coordinated methanol was retained. Thus, $n_{alcohol} = n_{catalyst}$ for **3a** and **5a**·MeOH and $n_{alcohol} = 0$ for **3b**. Values were rounded to ±0.5 kg/mol. [c] Determined by GPC (see experimental part). Values were rounded to ±0.5 kg/mol.

Complex **5a**·MeOH showed less evidence of catalyst decomposition and polymerizations continue after 2 h to reach appr. 90% conversion after 4 h of reaction. The greater rigidity of the pyridyl-containing metallacycle in **5a**·MeOH might be responsible for the enhanced thermal stability. Assuming the typically observed first-order dependence of the rate on lactide concentration, the curvature of the logarithmic plot of conversion vs. time indicates slow polymerization initiation (Fig. S1), but the general experimental error is too large to draw a definitive conclusion. Polymerizations with **5a**·MeOH showed narrow polydispersities of 1.1 – 1.3 at 2 h reaction time and 50% conversion, which increased to 1.4 – 1.6 at 4 h and 90% conversion (Table 2). The latter is indicative of transesterification side reactions, which become more evident at higher conversions. MALDI spectra of polymers obtained with **5a**·MeOH after 2 and 4 h showed indeed a series of peaks with $\Delta m/z = 72$, indicative of transesterification reactions (Fig. S2). The intensity of peaks originating from transesterification increases in the polymer obtained after 4 h of polymerization, in agreement with the observed increase of polydispersity. PLA produced by all three complexes was atactic to slightly heterotactic (**3a**: P_r = 0.67-0.68 (lactide:Mn = 300:1), **3b**: 0.70-0.73 (200:1), **5a**: 0.60-0.62 (300:1)).

Given the air-stability of the complexes, it seemed of interest to verify the performance of **5a**·MeOH under less rigorous exclusion of moisture. Thus a sample of **5a**·MeOH was washed with water, dried and used in *rac*-lactide polymerization under standard conditions (Table 3). The activity was only slightly lower than that of the untreated catalyst and polydispersities remained narrow. Obtained polymer molecular weights showed a lower number of polymer chains produced per manganese, which might indicate (partial) loss of coordinated methanol upon washing. Alternatively, three equivalents of water were added to polymerizations with **5a**·MeOH without any notable effect on polymerization activity. Polymerization of unpurified lactide resulted in a more drastic decrease of polymerization activity and only 26% conversion was observed after 4 h (Table 3). Narrow polydispersities and good agreements of expected and calculated polymer molecular weights indicate that coordinated methanol and methoxide are liberated upon catalyst degradation. The most likely deactivation path is thus protonation of the methoxide in **5a**·MeOH by lactic acid to form a less reactive/unreactive lactate complex. Polymerization with purified lactide under ambient atmosphere proceeded with a comparable loss of activity (Table 3). An increased number of polymer chains per manganese indicate that water absorbed from the atmosphere might act as a chain-transfer reagent.

Table 3. *Rac*-lactide polymerization with **5a**·MeOH in the presence of protic impurities [a]

Conditions	Reaction time / h	Conversion · 100	M_n (calc.) · mol/kg [b]	M_n (GPC) · mol/kg [c]	M_w/M_n	Polymer chains per Mn [d]
Purified lactide,	2	46	12	12	1.3	2.0
sealed tube under N_2	4	88	19	16	1.6	2.3
Catalyst washed with H_2O, purified	2	14	3	4	1.3	1.6
lactide, sealed tube under N_2	4	70	15	29	1.3	1.0
Unpurified lactide,	2	12	2.5	4.5	1.1	1.2
sealed tube under N_2	4	26	6	6	1.1	1.9
Purified lactide,	2	8	3.5	0.5	1.0	6.5
ambient atmosphere	4	38	8.5	3.5	1.1	4.8

[a] Conditions: 130 °C, lactide:catalyst = 300:1. [b] Calculated from $m_{lactide}/(n_{catalyst}+n_{alcohol})$·conversion+$M_{MeOH}$, with $n_{alcohol} = n_{catalyst}$ [c] Determined by GPC (see experimental part). [d] Calculated from $(m_{lactide}/n_{catalyst}$·conversion+$M_{MeOH})/M_n$(GPC).

Dalton Transactions

ARTICLE

Lowered, but still notable activity in the presence of impurities might indicate a (reversible) deactivation by lactic acid (water might form dilactic acid on first insertion, Scheme 4) or that polymerization follows an activated-monomer mechanism instead of a coordination-insertion mechanism (Scheme 4). In fact, previous reports on Mn-catalyzed lactide polymerization employed catalyst structures lacking good initiating groups and are either likely[56, 57] or proven[38] to follow an activated-monomer mechanism.

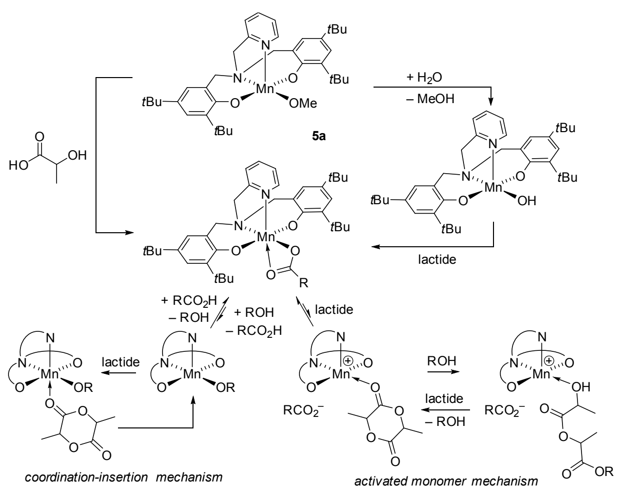

Scheme 4

To verify the presence of a coordination-insertion mechanism in the reactions studied here, the activity of **5a**·MeOH and its chloro-derivative **4a**·MeOH was investigated in the presence of varying amounts of external alcohol (Table 4). Employing methanol as external alcohol, advantageous since it is already present in the employed catalysts, led to variable results, probably due to competition between incorporation of methanol in the polymer chain and its evaporation into the head space of the reaction. Additional experiments were thus conducted using benzyl alcohol. Overall, the activity of **5a**·MeOH is significantly higher than that of **4a**·MeOH. The opposite would have been expected for an activated-monomer mechanism, which should favour the more Lewis-acidic **4a**·MeOH. Further, the activity of **5a**·MeOH remained unchanged upon addition of five equivalents of alcohol (Table 4). Polymerizations with **5a**·MeOH thus clearly follow a coordination-insertion mechanism. Catalyst **4a**·MeOH, on the other hand, shows increased conversions in the presence of external alcohol (Table 4). When large amounts of external alcohol were added (35-95 equiv), conversions of 90% were achieved in 30 min (Table S1). Polymerization of **4a**·MeOH are thus in agreement with simple Lewis-acid activation of the monomer. Activities observed for **4a**·MeOH are in the range of error comparable to those observed for **5a**·MeOH in the presence of protic impurities (Table 3) and both mechanisms are possible for the deactivated form of **5a**·MeOH.

Table 4. Effect of additional alcohol on *rac*-lactide conversion at different reaction times [a]

Time / min	**5a**·MeOH	**5a**·MeOH + 5 BnOH	**4a**·MeOH	**4a**·MeOH + 5 BnOH
30	7 – 18 (2)	17	5 – 10 (3)	
60		19 – 27 (2)	6	16 – 22 (2)
120	51	30	7	32
240	88	95		43
Time / min	**4a**·MeOH	**4a**·MeOH + 1 MeOH	**4a**·MeOH + 2 MeOH	**4a**·MeOH + 1 NaOMe
15	7 – 8 (2)	4 – 18 (3)	4 – 49 (4)	
30	5 – 10 (3)	0 – 8 (4)	14 – 47 (2)	
60	6		17 – 61 (3)	27
120	7		39 – 88 (2)	13

[a] Conversion in %, numbers in parenthesis indicate the number of polymerization experiments. Conditions: *rac*-lactide : catalyst = 200 : 1, 130 °C, sealed tube.

Polymerization of **4a**·MeOH in the presence of sodium methoxide was expected to provide activities comparable to the directly prepared methoxide derivative. Activities remained, however, well below those of to **5a**·MeOH (Table 4), indicating that in-situ preparation of the active species is inefficient in this system. Complex **4b**·MeOH was likewise applied to the polymerization of lactide in the presence of either 2 equivalents of methanol or one equivalent of sodium methoxide, but proved to be unreactive (< 7% conversion after 1 or 2 h, Table S1).

Conclusions

Manganese complexes of type **A** (Scheme 1) are air-stable and are moderately active catalysts for the polymerization of *rac*-lactide. While neither of the presented catalysts represents a significant improvement over existing systems using other metal centers, they compare well to other Mn-based catalysts. Polymerization activities were higher than those of simple MnX_2 salts, such as $MnCl_2$ or $Mn(OAc)_2$,[56, 57] which required several days at 145 °C. In the presence of larger amounts of external alcohol and following an activated monomer mechanism,[57] activities were similar to those observed for **4a**·MeOH. For **5a**·MeOH, polymerization was shown to proceed via a coordination-insertion mechanism.

Polymerization activities were similar to the Mn salen chloride catalyst reported by Idage,[38] for which the polymerization mechanism is unclear. Although reports on lactide polymerization with Mn so far do not indicate a significant advantage of Mn over other mid-range transition metals, the observed coordination-insertion mechanism offers the chance to improve catalyst activity and polymer molecular weight control for manganese-based catalysts by correct choice of ligand design.

EXPERIMENTAL SECTION

General considerations. Ligand and complex synthesis was performed under ambient atmosphere. Polymerization reactions were carried out under N_2 atmosphere in a sealed tube if not stated otherwise. Ligands **1a-1c** and **2a-2c** were prepared following literature protocols with small variations in some cases:[75-77] **1a**, **2a**: reflux for 24 h instead of reaction at ambient temperature; **1c**, **2c**: reflux in water for 24 h instead of methanol. *rac*-Lactide (98%) was purchased from Sigma–Aldrich, purified by 3x recrystallization from dry ethyl acetate and kept at –30 °C. All other chemicals were purchased from common commercial suppliers and used without further purification. ^{1}H spectra were acquired on a Bruker AVX 400 spectrometer. The chemical shifts were referenced to the residual signals of the deuterated solvents ($CDCl_3$: ^{1}H: δ 7.26 ppm). Magnetic moments were determined using the Evans method at ambient temperature in 10% $SiMe_4$/MeOD.[72, 73] Elemental analyses were performed by the Laboratoire d'analyse élémentaire (Université de Montréal). Most compounds contained co-crystallized solvent according to the X-ray diffraction analyses, but combustion analysis indicated that these solvents were mostly removed on drying (see sup. information).

(tBu$_2$ArO-CH$_2$)$_2$N(C$_2$H$_4$NMe$_2$)Mn(OMe), 3a. Ligand **1a** (0.52 g, 0.99 mmol) was added to a solution of $MnCl_2$ (0.13 g, 1.0 mmol) in methanol (30 ml) and stirred at ambient temperature for 1 h. A solution of NaOH (40 mg, 0.7 mmol) in MeOH (7 ml) was then added dropwise. Stirring was continued for another hour. The obtained solution was concentrated to 1/3 of its volume to yield purple crystals (546 mg, 86%).

Anal. Calcd for $C_{35}H_{57}MnN_2O_3\cdot MeOH$: C, 67.47; H, 9.60; N, 4.37. Found C, 67.00; H, 9.26; N, 4.44. (One molecule of co-crystallized methanol was observed in the crystal structure.) UV/vis (MeOH, $1.64\cdot10^{-4}$ mol/L) [λ_{max}, nm (ε, mol^{-1} cm^2)]: 278 (19 000), 330 (sh, 4900), 381 (5100), 512 (3100). μ_{eff}(MeOD) = 4.4 μ_B.

(Cl$_2$ArO-CH$_2$)$_2$N(C$_2$H$_4$NMe$_2$)Mn(OMe), 3b. Analogous to **3a**, ligand **1b** (0.39 g, 0.89 mmol), $MnCl_2$ (0.11 g, 0.90 mmol) and NaOH (36 mg, 0.9 mmol) in methanol (7 ml) afforded **3b** as brown powder (223 mg, 48%).

Anal. Calcd for $C_{19}H_{21}Cl_4MnN_2O_3$: C, 43.71; H, 4.05; N, 5.37. Found : C, 43.35; H, 3.67; N, 5.38. UV/vis (MeOH, $1.92\cdot10^{-4}$ mol/L) [λ_{max}, nm (ε, mol^{-1} cm^2)]: 293 (5500), 370 (sh, 1600), 484 (700), 735 (150). μ_{eff}(MeOD) = 4.6 μ_B.

(tBu$_2$ArO-CH$_2$)$_2$N(CH$_2$C$_6$H$_4$N)MnCl(MeOH), 4a·MeOH. Analogous to **3a**, ligand **2a** (0.48 g, 0.88 mmol), $MnCl_2$ (0.11 g, 0.90 mmol) and NaOMe (100 mg, 1.8 mmol) in methanol (7 ml) afforded **4a**·MeOH as purple crystals (481 mg, 82%).

Anal. Calcd for $C_{36}H_{50}ClMnN_2O_2\cdot MeOH_{0.5}$: C, 67.53; H, 8.07; N, 4.31. Found: C, 67.72; H, 8.14; N, 4.29. (Co-crystallized solvent observed in X-ray structure, but partly lost on drying.) UV/vis (MeOH, $1.51\cdot10^{-4}$ mol/L) [λ_{max}, nm (ε, mol^{-1} cm^2)]: 259 (16 000), 376 (4500), 518 (2600). μ_{eff}(MeOD) = 4.3 μ_B.

(Cl$_2$ArO-CH$_2$)$_2$N(CH$_2$C$_6$H$_4$N)MnCl(MeOH), 4b·MeOH. Ligand **2b** (0.38 g, 0.83 mmol) was added to a solution of $MnCl_2$ (0.11 g, 0.90 mmol) in methanol (30 ml) and stirred for 1 h. A solution of NaOMe (100 mg, 1.8 mmol) in methanol (7 ml) was added dropwise and the reaction heated at reflux for 12 h. The resulting solution was cooled to room temperature and concentrated to 1/3 of its volume to yield red crystals (364 mg, 76%).

Anal. Calcd for $C_{21}H_{18}Cl_5MnN_2O_3$: C, 43.60; H, 3.14; N, 4.84. Found : C, 43.49; H, 2.95; N, 4.62. (Two additional molecules of methanol were found in the crystal structure, but lost on drying.) UV/vis (MeOH, $1.51\cdot10^{-4}$ mol/L) [λ_{max}, nm (ε, mol^{-1} cm^2)]: 302 (21 000), 360 (sh, 5500), 470 (sh, 2400), 760 (sh, 400). μ_{eff}(MeOD) = 4.2 μ_B.

(tBu$_2$ArO-CH$_2$)$_2$N(CH$_2$C$_6$H$_4$N)Mn(OMe)(MeOH), 5a·MeOH. Ligand **2a** (0.48 g, 0.88 mmol) was added to a solution of $MnCl_2$ (0.11 g, 0.90 mmol) in methanol (30 ml) and stirred for 1 h at ambient temperature. A solution of NaOMe (150 mg, 2.7 mmol) in methanol (10 ml) was added dropwise and stirring continued for one day. A second portion of NaOMe (50 mg, 0.90 mmol) in methanol (3 ml) was added dropwise and stirring continued for a further day. Concentration of the solution to 1/3 of its volume afforded after one day purple crystals of **5a**·MeOH (494 mg, 85%).

Anal. Calcd for $C_{38}H_{57}MnN_2O_4$: C, 69.07; H, 8.69; N, 4.24. Found : C, 69.10; H, 8.58; N, 4.34. UV/vis (MeOH, $1.64\cdot10^{-4}$ mol/L) [λ_{max}, nm (ε, mol^{-1} cm^2)]: 259 (24 000), 342 (sh, 7100), 410 (sh, 3600), 540 (sh, 1600). μ_{eff}(MeOD) = 4.5 μ_B.

Lactide polymerization. In a glovebox under an N_2 atmosphere, a pressure tube was charged with 400 – 450 mg of *rac*-lactide. The required amount of catalyst was added to obtain the desired catalyst loading of 0.33 – 1.0 mol-% and, if desired, several µL of a solution of MeOH or BnOH in toluene. The pressure tube was sealed, removed from the glove box and immersed in an oil bath pre-heated to 130 °C. The polymerization was conducted under light stirring for the desired time, the pressure tube removed from the oil bath and cooled for appr. 5 min. A solution of acetic acid in $CDCl_3$ (1 M, 3 – 4 drops) was added to quench the reaction. After cooling to room temperature, the polymer was dissolved in $CDCl_3$ and filtered through a short silica plug, which was rinsed with additional $CDCl_3$. In the absence of external alcohol, the solution was analyzed by NMR and then evaporated to dryness. In the presence of added alcohol, the solution was immediately evaporated and samples were re-dissolved for NMR analysis. All isolated polymers were kept at –80 °C between analyses.

Conversion was determined from ^{1}H NMR in $CDCl_3$ by comparison to remaining lactide. P_r was determined from decoupled ^{1}H NMR by $P_r = 2{\cdot}I_1/(I_1+I_2)$, with I_1 = 5.20 – 5.25 ppm (*rmr, mmr/rmm*), I_2 = 5.13 – 5.20 ppm (*mmr/rmm, mmm, mrm*). Molecular weight analyses were performed on a Waters 1525 gel permeation chromatograph equipped with three Phenomenex columns and a refractive index detector at 35 °C. THF was used as the eluent at a flow rate of 1.0 mL·min^{-1} and polystyrene standards (Sigma–Aldrich, 1.5 mg·mL^{-1}, prepared and filtered (0.2 mm) directly prior to injection) were used for calibration. Obtained molecular weights were corrected by a Mark-Houwink factor of 0.58.[78]

X-ray diffraction studies. Single crystals were obtained directly from isolation of the products as described above. Diffraction data were collected on a Bruker Microstar with a rotating anode source (Cu Kα), on a Bruker Smart APEX with a microsource (Cu Kα) or on a Bruker Venture metaljet diffractometer (Ga Kα) using the APEX2 software package.[79] Data reduction was performed with SAINT,[80] absorption corrections with SADABS.[81] Structures were solved using intrinsic phasing (SHELXT).[82] All non-hydrogen atoms were refined anisotropic using full-matrix least-squares on F^2 and hydrogen atoms refined with fixed isotropic U using a riding model (SHELXL97).[83] Only weakly diffracting crystals could be obtained for **4a**·MeOH and **5a**·MeOH, which resulted in increased R_σ and $R1$ values. Two strongly disordered co-crystallized methanol molecules could be identified, but not refined in **4b**·MeOH and were removed using the solvent mask routine in OLEX2. Disordered *tert*-butyl groups in **3a** and ***5a·MeOH*** were refined using appropriate restraints (SADI, RIGU). Complex **4a**·MeOH was found to be non-merohedrally twinned (80:20) and refined using an HKLF 5 file obtained from PLATON/TWINROTMAT.[84] Further experimental details can be found in Table 5 and in the supporting information (CIF).

Table 5. Details of X-ray diffraction studies

	3a	**4a**·MeOH	**4b**·MeOH	**5a**·MeOH
Formula	$C_{35}H_{57}MnN_2O_3{\cdot}MeOH$	$C_{37}H_{54}ClMnN_2O_3{\cdot}H_2O$	$C_{21}H_{18}Cl_5MnN_2O_3{\cdot}2$ MeOH	$C_{38}H_{57}MnN_2O_4{\cdot}MeOH$
M_w (g/mol); $d_{calcd.}$ (g/cm^3)	640.80; 1.180	683.22; 1.226	578.56; 1.549	692.83; 1.154
T (K); F(000)	150; 1392	150; 1464	100; 1312	150; 748
Crystal System	orthorhombic	monoclinic	monoclinic	triclinic
Space Group	$Pna2_1$	$P2_1/c$	$P2_1/c$	P-1
Unit Cell: a (Å)	12.3705(4)	15.2595(8)	12.7413(7)	10.5736(8)
b (Å)	10.8698(4)	15.9590(9)	13.0938(7)	12.2554(9)
c (Å)	26.8207(9)	15.8429(9)	16.8087(9)	16.4321(13)
α (°)				104.320(5)
β (°)		106.365(4)	100.589(2)	103.352(5)
γ (°)				92.336(5)
V (Å^3); Z	3606.4(2); 4	3701.9(4); 4	2756.5(3); 4	1996.6(3); 2
μ (mm^{-1}); Abs. Corr.	3.26; multi-scan	2.54; multi-scan	8.67; multi-scan	1.97; multi-scan
θ range (°); completeness	1.6 – 67.7; 1.00	3.5 – 60.9; 0.99	3.5 – 67.7; 1.00	3.3 – 53.6; 1.00
collected reflections; R_σ	71267; 0.038	50921; 0.13	38130; 0.030	33228; 0.078
unique reflections; R_{int}	6675; 0.053	8498; 0.19	5371; 0.049	9145; 0.087
observed reflections; R1(F)	6432; 0.039	4189; 0.100	4930; 0.039	5223; 0.073
wR(F^2) (all data); GoF(F^2)	0.078; 1.03	0.31; 1.038	0.112; 1.044	0.22; 1.03
Residual electron density	0.25; –0.32	1.1; –0.92	0.89; –0.71	0.65; –0.53

Acknowledgements

Support by Francine Bélanger (X-ray) and Marie-Christine Tang (MALDI) is gratefully acknowledged. Funding was supplied by the NSERC – Discovery Program.

Notes and references

1. S. Slomkowski, S. Penczek and A. Duda, *Polym. Adv. Technol.*, 2014, **25**, 436-447.
2. M. Singhvi and D. Gokhale, *RSC Advances*, 2013, **3**, 13558-13568.
3. A. Sauer, A. Kapelski, C. Fliedel, S. Dagorne, M. Kol and J. Okuda, *Dalton Trans.*, 2013, **42**, 9007-9023.
4. R. Jianming, X. Anguo, W. Hongwei and Y. Hailin, *Des. Monomers Polym.*, 2013, **17**, 345-355.
5. B. H. Huang, S. Dutta and C. C. Lin, in *Comprehensive Inorganic Chemistry II (Second Edition)*, ed. J. R. Poeppelmeier, Elsevier, Amsterdam, 2013, DOI: http://dx.doi.org/10.1016/B978-0-08-097774-4.00146-7, pp. 1217-1249.
6. S. Dagorne, M. Normand, E. Kirillov and J.-F. Carpentier, *Coord. Chem. Rev.*, 2013, **257**, 1869-1886.
7. J.-F. Carpentier, B. Liu and Y. Sarazin, in *Advances in Organometallic Chemistry and Catalysis*, John Wiley & Sons, Inc., 2013, DOI: 10.1002/9781118742952.ch28, pp. 359-378.

8. I. dos Santos Vieira and S. Herres-Pawlis, *Eur. J. Inorg. Chem.*, 2012, **2012**, 765-774.
9. S. Dutta, W.-C. Hung, B.-H. Huang and C.-C. Lin, in *Synthetic Biodegradable Polymers*, eds. B. Rieger, A. Künkel, G. W. Coates, R. Reichardt, E. Dinjus and T. A. Zevaco, Springer-Verlag, Berlin, 2011, pp. 219-284.
10. P. J. Dijkstra, H. Du and J. Feijen, *Polym. Chem.*, 2011, **2**, 520-527.
11. N. Ajellal, J.-F. Carpentier, C. Guillaume, S. M. Guillaume, M. Helou, V. Poirier, Y. Sarazin and A. Trifonov, *Dalton Trans.*, 2010, **39**, 8363.
12. M. D. Jones, in *Heterogenized Homogeneous Catalysts for Fine Chemicals Production*, eds. P. Barbaro and F. Liguori, Springer Netherlands, 2010, vol. 33, pp. 385-412.
13. A. K. Sutar, T. Maharana, S. Dutta, C.-T. Chen and C.-C. Lin, *Chem. Soc. Rev.*, 2010, **39**, 1724-1746.
14. C. M. Thomas, *Chem. Soc. Rev.*, 2010, **39**, 165.
15. J.-F. Carpentier, *Macromol. Rapid Comm.*, 2010, **31**, 1696-1705.
16. C. A. Wheaton, P. G. Hayes and B. J. Ireland, *Dalton Trans.*, 2009, 4832 - 4846.
17. H. Ma and J. Okuda, *Macromolecules*, 2005, **38**, 2665-2673.
18. A. Amgoune, C. M. Thomas, T. Roisnel and J.-F. Carpentier, *Chem.-Eur. J.*, 2006, **12**, 169-179.
19. E. M. Broderick and P. L. Diaconescu, *Inorg. Chem.*, 2009, **48**, 4701-4706.
20. Z. Zhang and D. Cui, *Chem.-Eur. J.*, 2011, **17**, 11520-11526.
21. C. Bakewell, T.-P.-A. Cao, N. Long, X. F. Le Goff, A. Auffrant and C. K. Williams, *J. Am. Chem. Soc.*, 2012, **134**, 20577-20580.
22. C.-Y. Tsai, H.-C. Du, J.-C. Chang, B.-H. Huang, B.-T. Ko and C.-C. Lin, *RSC Advances*, 2014, **4**, 14527-14537.
23. A. Stopper, J. Okuda and M. Kol, *Macromolecules*, 2012, **45**, 698-704.
24. C. A. Wheaton and P. G. Hayes, *Comments Inorg. Chem.*, 2011, **32**, 127-162.
25. M. Cheng, A. B. Attygalle, E. B. Lobkovsky and G. W. Coates, *J. Am. Chem. Soc.*, 1999, **121**, 11583-11584.
26. H. R. Kricheldorf and D.-O. Damrau, *Macromol. Chem. Phys.*, 1997, **198**, 1767-1774.
27. A. Södergård and M. Stolt, *Macromol. Symp.*, 1998, **130**, 393-402.
28. M. Stolt and A. Södergård, *Macromolecules*, 1999, **32**, 6412-6417.
29. B. J. O'Keefe, S. M. Monnier, M. A. Hillmyer and W. B. Tolman, *J. Am. Chem. Soc.*, 2001, **123**, 339-340.
30. V. C. Gibson, E. L. Marshall, D. Navarro-Llobet, A. J. P. White and D. J. Williams, *J. Chem. Soc., Dalton Trans.*, 2002, DOI: 10.1039/B209703F, 4321-4322.
31. B. J. O'Keefe, L. E. Breyfogle, M. A. Hillmyer and W. B. Tolman, *J. Am. Chem. Soc.*, 2002, **124**, 4384-4393.
32. D. S. McGuinness, E. L. Marshall, V. C. Gibson and J. W. Steed, *J. Polym. Sci., Part A: Polym. Chem.*, 2003, **41**, 3798-3803.
33. A. B. Biernesser, B. Li and J. A. Byers, *J. Am. Chem. Soc.*, 2013, **135**, 16553-16560.
34. C. M. Manna, H. Z. Kaplan, B. Li and J. A. Byers, *Polyhedron*, 2014, **84**, 160-167.
35. J. L. Gorczynski, J. Chen and C. L. Fraser, *J. Am. Chem. Soc.*, 2005, **127**, 14956-14957.
36. X. Wang, K. Liao, D. Quan and Q. Wu, *Macromolecules*, 2005, **38**, 4611-4617.
37. J. Chen, J. L. Gorczynski, G. Zhang and C. L. Fraser, *Macromolecules*, 2010, **43**, 4909-4920.
38. B. B. Idage, S. B. Idage, A. S. Kasegaonkar and R. V. Jadhav, *Mater. Sci. Eng., B*, 2010, **168**, 193-198.
39. Y. Y. Kang, H.-R. Park, M. H. Lee, J. An, Y. Kim and J. Lee, *Polyhedron*, 2015, **95**, 24-29.
40. A. Keuchguerian, B. Mougang-Soume, F. Schaper and D. Zargarian, *Can. J. Chem.*, 2015, **93**, 594–601.
41. A. Kundys, A. Plichta, Z. Florjańczyk, A. Frydrych and K. Żurawski, *J. Polym. Sci., Part A: Polym. Chem.*, 2015, **53**, 1444-1456.
42. A. C. Silvino, A. L. C. Rodrigues and J. A. L. C. Resende, *Inorg. Chem. Commun.*, 2015, **55**, 39-42.
43. J. Sun, W. Shi, D. Chen and C. Liang, *J. Appl. Polym. Sci.*, 2002, **86**, 3312-3315.
44. A. John, V. Katiyar, K. Pang, M. M. Shaikh, H. Nanavati and P. Ghosh, *Polyhedron*, 2007, **26**, 4033-4044.
45. S. Bhunora, J. Mugo, A. Bhaw-Luximon, S. Mapolie, J. Van Wyk, J. Darkwa and E. Nordlander, *Appl. Organomet. Chem.*, 2011, **25**, 133-145.
46. L.-L. Chen, L.-Q. Ding, C. Zeng, Y. Long, X.-Q. Lü, J.-R. Song, D.-D. Fan and W.-J. Jin, *Appl. Organomet. Chem.*, 2011, **25**, 310-316.
47. R. R. Gowda and D. Chakraborty, *J. Molec. Catal. A: Chem.*, 2011, **349**, 86-93.
48. T. J. J. Whitehorne and F. Schaper, *Chem. Commun. (Cambridge, U. K.)*, 2012, **48**, 10334-10336.
49. T. J. J. Whitehorne and F. Schaper, *Inorg. Chem.*, 2013, **52**, 13612-13622.
50. T. J. J. Whitehorne and F. Schaper, *Can. J. Chem.*, 2014, **92**, 206-214.
51. T. J. J. Whitehorne, B. Vabre and F. Schaper, *Dalton Trans.*, 2014, **43**, 6339-6352.
52. K. S. Kwon, J. Cho, S. Nayab and J. H. Jeong, *Inorg. Chem. Commun.*, 2015, **55**, 36-38.
53. A. Routaray, N. Nath, T. Maharana and A. k. Sutar, *J. Macromol. Sci., Part A: Pure Appl.Chem.*, 2015, **52**, 444-453.
54. S. Fortun, P. Daneshmand and F. Schaper, *Angew. Chem., Int. Ed. Engl.*, 2015, **in print**, 10.1002/ange.201505674.
55. V. Balasanthiran, C. Chatterjee, M. H. Chisholm, N. D. Harrold, T. V. RajanBabu and G. A. Warren, *J. Am. Chem. Soc.*, 2015, **137**, 1786-1789.
56. H. R. Kricheldorf and D.-O. Damrau, *J. Macromol. Sci., Part A: Pure Appl.Chem.*, 1998, **35**, 1875-1887.
57. B. Rajashekhar and D. Chakraborty, *Polym. Bull.*, 2014, **71**, 2185-2203.
58. L. Ding, W. Jin, Z. Chu, L. Chen, X. Lü, G. Yuan, J. Song, D. Fan and F. Bao, *Inorg. Chem. Commun.*, 2011, **14**, 1274-1278.
59. W.-J. Jin, L.-Q. Ding, Z. Chu, L.-L. Chen, X.-Q. Lü, X.-Y. Zheng, J.-R. Song and D.-D. Fan, *J. Molec. Catal. A: Chem.*, 2011, **337**, 25-32.
60. G. Xiao, B. Yan, R. Ma, W. J. Jin, X. Q. Lu, L. Q. Ding, C. Zeng, L. L. Chen and F. Bao, *Polym. Chem.*, 2011, **2**.
61. S. Gendler, S. Segal, I. Goldberg, Z. Goldschmidt and M. Kol, *Inorg. Chem.*, 2006, **45**, 4783-4790.
62. Z. Tang and V. C. Gibson, *European Polymer Journal*, 2007, **43**, 150-155.

63. X. Liu, X. Shang, T. Tang, N. Hu, F. Pei, D. Cui, X. Chen and X. Jing, *Organometallics*, 2007, **26**, 2747-2757.
64. H. E. Dyer, S. Huijser, A. D. Schwarz, C. Wang, R. Duchateau and P. Mountford, *Dalton Trans.*, 2008, DOI: 10.1039/B714583G, 32-35.
65. M. Hirotsu, M. Kojima and Y. Yoshikawa, *Bull. Chem. Soc. Jpn.*, 1997, **70**, 649-657.
66. M. Hirotsu, M. Kojima, W. Mori and Y. Yoshikawa, *Bull. Chem. Soc. Jpn.*, 1998, **71**, 2873-2884.
67. E. Chard, L. N. Dawe and C. M. Kozak, *Acta Crystallogr., Sect. E: Struct. Rep. Online*, 2010, **66**, m771.
68. R. van Gorkum, J. Berding, A. M. Mills, H. Kooijman, D. M. Tooke, A. L. Spek, I. Mutikainen, U. Turpeinen, J. Reedijk and E. Bouwman, *Eur. J. Inorg. Chem.*, 2008, **2008**, 1487-1496.
69. D. Maity, W. S. Sheldrick, H. M.-F. Mayer-Figge and M. Ali, *Indian J. Chem., Sect A*, 2007, **46**, 1057-1062.
70. N. Noshiranzadeh, M. Emami, R. Bikas, K. Ślepokura and T. Lis, *Polyhedron*, 2014, **72**, 56-65.
71. N. Reddig, D. Pursche, B. Krebs and A. Rompel, *Inorg. Chim. Acta*, 2004, **357**, 2703-2712.
72. D. F. Evans, *J. Chem. Soc.*, 1959, DOI: 10.1039/JR9590002003, 2003-2005.
73. E. M. Schubert, *J. Chem. Educ.*, 1992, **69**, 62.
74. F. H. Allen, *Acta Crystallogr., Sect. B: Struct. Sci.*, 2002, **B58**, 380-388.
75. E. Y. Tshuva, I. Goldberg, M. Kol and Z. Goldschmidt, *Organometallics*, 2001, **20**, 3017-3028.
76. S. Groysman, I. Goldberg, M. Kol, E. Genizi and Z. Goldschmidt, *Organometallics*, 2004, **23**, 1880-1890.
77. A. J. Nielson and J. M. Waters, *Polyhedron*, 2010, **29**, 1715-1726.
78. M. Save, M. Schappacher and A. Soum, *Macromol. Chem. Phys.*, 2002, **203**, 889-899.
79. *Journal*, 2006, Bruker Molecular Analysis Research Tool.
80. *Journal*, 2006, Integration Software for Single Crystal Data.
81. G. M. Sheldrick, *Journal*, 1996 & 2004, Bruker Area Detector Absorption Corrections.
82. G. Sheldrick, *Acta Crystallographica Section A*, 2015, **71**, 3-8.
83. G. M. Sheldrick, *Acta Crystallogr.*, 2008, **A64**, 112-122.
84. A. Spek, *Acta Cryst. D*, 2009, **65**, 148-155.

Graphical Abstract

Diamino-diphenolato manganese(III) complexes polymerize *rac*-lactide via a coordination-insertion or an activated monomer mechanism, depending on the ancillary ligand.